ResearchGate

See discussions, stats, and author profiles for this publication at: https://www.researchgate.net/publication/24255565

Spacer Site Modifications for the Improvement of the in Vitro and in Vivo Binding Properties of Tc-99m-N3S-X-Bombesin[2-14] Derivatives

ARTICLE *in* BIOCONJUGATE CHEMISTRY · APRIL 2009

Impact Factor: 4.51 · DOI: 10.1021/bc800475k · Source: PubMed

CITATIONS
20

READS
34

12 AUTHORS, INCLUDING:

Penelope Bouziotis
National Center for Scientific Research De…
58 PUBLICATIONS **448** CITATIONS
SEE PROFILE

Evangelia Livaniou
National Center for Scientific Research De…
72 PUBLICATIONS **979** CITATIONS
SEE PROFILE

Alexandra Varvarigou
National Center for Scientific Research De…
81 PUBLICATIONS **1,153** CITATIONS
SEE PROFILE

Available from: Eirini Fragogeorgi
Retrieved on: 02 February 2016

Spacer Site Modifications for the Improvement of the *in Vitro* and *in Vivo* Binding Properties of ^{99m}Tc-N_3S-X-Bombesin[2−14] Derivatives

Eirini A. Fragogeorgi,[†] Christos Zikos,[†,‡] Eleni Gourni,[†] Penelope Bouziotis,[†] Maria Paravatou-Petsotas,[†] George Loudos,[§] Nikolaos Mitsokapas,[†] Stavros Xanthopoulos,[†] Mary Mavri-Vavayanni,[||] Evangelia Livaniou,[†] Alexandra D. Varvarigou,[†] and Spyridon C. Archimandritis*[,†]

Institute of Radioisotopes-Radiodiagnostic Products, National Center for Scientific Research "Demokritos", 15310 Aghia Paraskevi, Athens, Greece, Biomedica Life Sciences S.A. 15231, Athens, Greece, Technological Educational Institute of Athens, Athens, Greece, and Ethnikon kai Kapodistriakon Panepistimion Athinon, Greece. Received October 31, 2008; Revised Manuscript Received February 25, 2009

It has been shown that gastrin releasing peptide receptors (GRPRs) are overexpressed in various types of cancer cells. Bombesin is an analogue of the mammalian GRP that binds with high specificity and affinity to GRPRs. Significant research efforts have been lately devoted to the design of radiolabeled 8 or 14 aminoacid bombesin (BN) peptides for the detection (either with gamma or positron emitting radionuclides) and therapy (with β^- emitting radionuclides) of cancer. The specific aim of the present study was to further investigate the radiolabeled peptide structure and to determine whether the total absence of a linker or the use of a basic diverse amino acid linker could influence the biodistribution profile of the new compounds for specific targeting of human prostate cancer. Thus, two new derivatives with the structure Gly-Gly-Cys-X-BN[2−14], where linker X is either zero (I) or Orn-Orn-Orn (Orn: ornithine) (II) were designed and synthesized. The corresponding ^{99m}Tc-BN derivatives were obtained with high radiochemical yield (>98%) and had almost identical retention times in RP-HPLC with the $^{185/187}$Re complexes, which were also characterized by ESI-MS. Metabolic stability was found to be high in human plasma, moderate in PC-3 cells, and rather low in mouse liver and kidney homogenates for both BN derivatives studied. The BN derivative without the spacer was less stable in cell culture and liver homogenates. A satisfactory binding affinity to GRPRs, in the nanomolar range, was obtained for both BN derivatives as well as for their Re complexes, with BN (II) demonstrating the highest one. *In vitro* internalization/externalization assays indicated that ∼6% of BN (I) and ∼25% of BN (II) were internalized into PC-3 cells. *In vivo* evaluation in normal Swiss mice and in tumor bearing SCID mice showed that BN (II) presented higher tumor and pancreas uptake than BN (I). Small animal SPECT dynamic imaging, carried out after an injection of BN (II) in mice bearing PC-3 tumors, resulted in PC-3 tumor delineation with low background activity. Overall, this study performed for two new N_3S-X-BN[2−14] derivatives indicated that hydrophilicity and charge strongly affected the *in vitro* and *in vivo* binding properties and the biodistribution pattern. This finding is confirmed by SPECT imaging of BN (II), which is under further *in vivo* evaluation for detecting cancer-positive GRPRs.

INTRODUCTION

Bombesin, BN, is an active 14-amino acid neuropeptide (pGlu[1]-Gln[2]-Arg[3]-Leu[4]-Gly[5]-Asn[6]-Gln[7]-Trp[8]-Ala[9]-Val[10]-Gly[11]-His[12]-Leu[13]-Met[14]) originally isolated from the skin of the European frog *Bombina bombina* (*1*). Four bombesin receptors, for bombesin and its derivatives belonging to the G-protein receptor superfamily, have been cloned: NMB- receptor (NMBr or BB1), GRP receptor (GRPR or BB2), BN receptor (BRSr or BB3 or orphan), and BN receptor subtype 4 (BB4) (*2, 3*).

The bombesin mammalian counterpart, named gastrin-releasing peptide, GRP, is a 27-amino acid peptide sharing the same C-terminal heptapeptide with bombesin. This C-terminal BN 7−14 amino acid sequence (Gln[7]-Trp[8]-Ala[9]-Val[10]-Gly[11]-His[12]-Leu[13]-Met[14]) is considered to be essential for peptide biological activity and receptor binding affinity. Consequently, GRP and BN have essentially identical physiologic action (*4, 5*). The GRP receptor is widely expressed not only in the central nervous system and the gastrointestinal and respiratory tracts, where important physiologic functions take place, but is also found aberrantly in human malignancies including prostate, pancreatic, lung, breast, gastrointestinal, and colorectal carcinomas as well as in small cell lung cancer (*6, 7*). This overexpression in various neoplasias in reference to normal tissues, combined with the ability of GRPR agonists to be internalized, has led to the development of BN-based radiopharmaceuticals (*8*). In the majority of the studies, BN[7−14], which serves as a highly specific GRP-receptor binding motif, has been selected and radiolabeled with a variety of SPECT, PET, and therapeutical radionuclides (*9*). Most radiolabeled, BN-like peptides with substitutions or deletions at the 7−14 amino acid sequence (important for conferring agonistic or antagonistic properties) are N-terminally attached via various spacer arms or linkers to the radioisotope-chelating moiety.

Several peptide structures that provide stable ^{99m}Tc complexes attached on the N-terminal region of BN derivatives have been investigated. Garcia Garayoa et al. (*10−12*) reported the design and development of organometallic Re/^{99m}Tc$(CO)_3^{(I)}$ BN analogues by introducing non-natural amino acids and different spacers in the BN (7−14) sequence. It was concluded by the above study that the insertion of spacers had a clear influence on peptide uptake both in healthy organs and in tumors, leaving

* To whom correspondence should be addressed. Tel: +30(210) 6503685. Fax: +30(210) 6522661. E-mail: sarxim@rrp.demokritos.gr.
[†] National Center for Scientific Research "Demokritos".
[‡] Biomedica Life Sciences S.A. 15231.
[§] Technological Educational Institute of Athens.
[||] Ethnikon kai Kapodistriakon Panepistimion Athinon.

10.1021/bc800475k CCC: $40.75 © 2009 American Chemical Society
Published on Web 04/03/2009

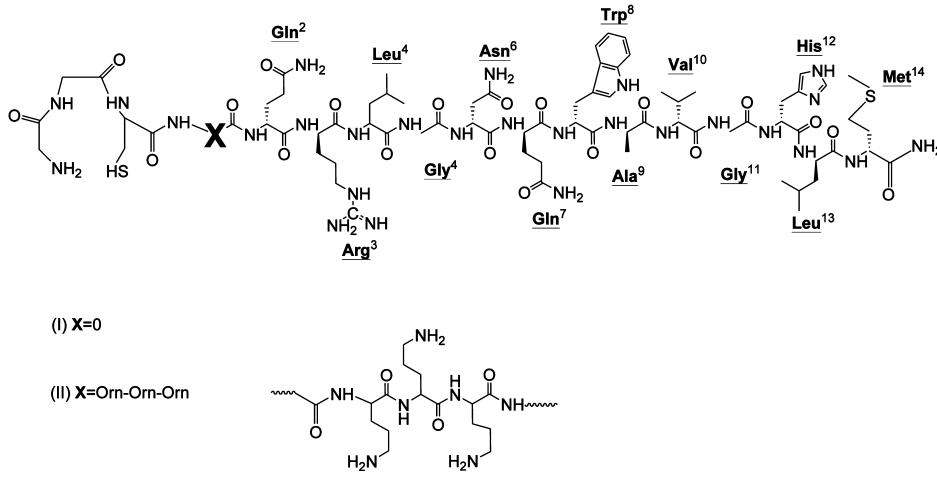

Figure 1. Structure and amino acid sequences of N_3S-X-BN[2−14] derivatives. BN(I): X = 0 (no spacer). BN(II): X = Orn-Orn-Orn.

the stability or receptor affinity unaffected. Smith et al. have studied ^{99m}Tc-complexes containing N_3S (*13*), tricarbonyl (*14, 15*), pyrazolyl (*16*), and "4 + 1" mixed ligand systems (*17*), N-terminally conjugated to BN(7−14) either directly or via spacer groups such as β-Ala, 5-Ava, 8-Aoc, 11-Aun, SSS, GGG, GSG, NNN, NNN-β-Ala, NNN-5-Ava, RRR, RRR- β-Ala, and RRR-5-Ava. Apart from ^{99m}Tc, which is among the most preferred radionuclides for imaging of the GRPR, for the design of BN-based radiopharmaceuticals labeled either with diagnostic [^{64}Cu (*18*−*21*), ^{68}Ga (*22*), ^{18}F (*23*), and ^{111}In (*24, 25*)] or therapeutic radioisotopes (^{64}Cu, ^{149}Pm, ^{153}Sm, ^{177}Lu, ^{90}Y, ^{111}In, and ^{188}Re) (*26*−*30*), BN structural modifications were also tried by the insertion of aliphatic, aminoacid, poly(ethyleneglycol), ether, and aromatic linking moieties. The main goal of all these efforts was to evaluate to what extent the length and the structure of the spacer or linking group would influence radiochemistry, metabolic stability, GRPR binding affinity, residualization of radioactivity in cancer cells, and pharmacokinetics of the labeled derivatives.

A traditional approach for radiolabeling BN derivatives with ^{99m}Tc is via stabilization of the $Tc^{(V)}O^{3+}$ metal core with ligands of the so-called N_3S type (*31*−*33*). Recently, our group (*34*) has focused on the design of BN derivatives in which the chelating moiety comprised a combination of amino acids X-Gly-Cys, where (X = Gly, methylglycine, dimethylglycine, and mercaptoacetic acid) N-terminally conjugated to the almost full length BN peptide, BN[2−14], through the hydrocarbon spacer arm Aca (6-aminohexanoic acid). A further comparative *in vivo* investigation (*35*) between the most promising derivative Gly-Gly-Cys-Aca-BN[2−14], resulting from the above study, and Gly-Gly-Cys-Aca-BN[7−14] showed that peptide chain length influenced the biodistribution of ^{99m}Tc-labeled derivatives. Taking into consideration the non-negligible liver uptake obtained with the peptides containing the six-carbon spacer, we further focused on the design of two novel BN[2−14]NH_2-like peptides. More specifically, the aliphatic spacer Aca was either eliminated or replaced by the non-natural basic amino acid sequence Orn-Orn-Orn (Orn = ornithine) (Figure 1). Previous studies of radiolabeled BN derivatives containing 3-, 5-, 8-, or 11-carbon spacers between the peptide and the chelator demonstrated that shortening the linker length liver uptake was reduced and pancreas was increased in nontumor bearing mice (*13*). Such considerations, together with an effort to make a full structure−activity relationship study, led us to the selection of a zero spacer in the case of BN (I) and of a more polar, charged linker in the case of BN (II). To the best of our knowledge, there are no other studies that have evaluated radiolabeled BN derivatives consisting of the BN[2−14] sequence conjugated to an N_3S chelator via no spacer or via a spacer containing the triaminoacid sequence of ornithines. The choice of three Orn as a spacer was made because we wanted to maximize the effect of the charge and thus to investigate whether, with the introduction of this polar linker in reference to no spacer, the hydrophilic character of the final compound dictates the biodistribution profile.

In the frame of the present study, the new BN derivatives were complexed with both ^{99m}Tc and $^{185/187}$Re(V) gluconate precursors. The nonradioactive rhenium complexes were characterized by liquid chromatography−electrospray ionization mass spectrometry (ESI-MS). Radiochemical identification, metabolic stability studies, *in vitro* assays including binding affinity, internalization/efflux studies as well as *in vivo* evaluation in normal Swiss mice and tumor (human prostate PC-3) bearing SCID mice are reported. The aim was to examine whether the modification of the spacer affected stability, affinity, lipophilicity, and the overall charge of the resulting ^{99m}Tc-BN derivatives and as a consequence the influence these changes exert on the *in vivo* profile of the resulting radiolabeled species.

EXPERIMENTAL PROCEDURES

Materials. The Fmoc-protected amino acids were purchased from the Chemical and Biopharmaceutical Laboratories (Patras, Greece), while the polystyrene resin was commercially available from Nova Biochem. Electrospray mass spectrum analyses were performed in the Mass Spectrometry and Dioxin Analysis Laboratory of NCSR "Demokritos". ^{99m}Tc, obtained in physiological saline as $Na^{99m}TcO_4$, was eluted from a commercial ^{99}Mo/^{99m}Tc generator (Mallinckrodt Medical, Petten, The Netherlands). The human prostate adenocarcinoma cell line was obtained from the American Type Culture Collection (ATCC). The product [^{125}I-Tyr^4]BN was purchased from Perkin-Elmer (Life Science Products, Boston MA, USA, Inc.; specific activity, 81.4 TBq/mmol, 10 μCi). Biodistribution studies were performed using female normal Swiss and SCID (severely compromised immunodeficient) mice (15−25 g) of the same colony and age, purchased from the Breeding Facilities of NCSR Demokritos. Reagents and media for cell culture were purchased from PAA Laboratories GmbH (Austria), and all other chemicals from Merck (Whitehouse Station, NJ 08889-0100 USA).

Instrumentation. Analytical reverse phase high performance liquid chromatography (RP-HPLCs) were performed on a Waters HPLC system (pump 616, detector 996 PDA) using a Hibar Pre-Packed Column RT 250−4, LiChrospher 100 RP-18 (5 μm) (250 mm, ID 4 mm, Merck). Semipreparative RP-HPLC was performed on a Waters (Milford, MA, USA) HPLC system

(pump 600E, detector UV-484). A 10 Nucleosil 7 C18 column [250 × 12.7 mm ID; Macherey-Nagel (Dueren, Germany)] was used. For (ESI-MS) mass spectral analysis, the test solution in 50% aqueous acetonitrile was infused into an electrospray interface mass spectrometer (AQA Navigator, Finnigan) at a flow rate of 0.1 mL/min, using a Harvant Syringe pump. Negative or positive ion ESI spectra were acquired by adjusting the needle and cone voltages accordingly. Hot nitrogen gas (Dominic-Hunter UHPLCMS-10) was used for desolvation at 170 °C. Instant thin layer chromatography (ITLC) measurements were made by electronic autoradiography (Instant Imager Packard-Canberra). Gamma decay detection of ^{125}I for the *in vitro* cell binding studies was performed on a γ counter (Model LB2111, Berthold detection system, Bad Wildbad, Germany). For internalization, efflux, and *in vivo* studies a multisample γ-counter system Packard Minaxi 5500 equipped with a 3″ NaI (Tl) crystal was used. Scintigraphic images were acquired on a pair of two square H8500 flat-panel PSPMT gently coupled to a NaI(Tl) crystal array (Bicron-St. Gobain), equipped with a parallel-hole lead collimator.

Solid Phase Peptide Synthesis. The BN derivatives were synthesized manually on a Rink-amide resin employing the Fmoc strategy as follows: Briefly, for coupling, an excess of Fmoc-protected amino acid and HOB*t* were dissolved in *N*,*N*′-dimethylformamide (DMF). The solution was cooled in ice, and then *N*,*N*′-diisopropylcarbodiimide (DIPC) was added. The reaction mixture was initially left for 10 min on ice, then for another 10 min at room temperature, and was finally added to the resin. The coupling efficiency was monitored by the Kaiser ninhydrin test (*36*). Removal of the N-terminal Fmoc group was achieved by repetitive treatment with 20% piperidine in DMF. The final product was cleaved from the resin using a cocktail of trifluoroacetic acid (TFA), thioanisol, ethanediol, phenol, H_2O, and triisopropylsilane (81.5/5/2.5/5/5/1, v/v/v/v/v/v). The crude product, obtained by precipitation with cold diethylether, was purified by semipreparative RP-HPLC. Elution was performed with a solvent system consisting of 0.05% TFA in water (solvent A) and 60% CH_3CN in solvent A (solvent B), by applying a linear gradient from 100% to 20% A in 47 min for BN (I) or from 100% to 50% A in 47 min for BN (II). The flow rate was 4.5 mL/min, and the peptide peaks were detected with a UV detector at 220 nm.

Conjugation of $^{185/187}$Re$^{(V)}$O-N$_3$S-BN Derivatives (Non-radioactive Complexes). Rhenium$^{(V)}$ oxo complexes of BN derivatives were prepared by ligand exchange reactions, starting from the preformed Re$^{(V)}$O gluconate precursor (*37*). An aqueous solution of both crude BN derivatives (10 and 20 mg, respectively) and a Re$^{(V)}$O gluconate solution were allowed to react at 60 °C for 2 h. The crude products were purified by semipreparative RP-HPLC. Elution was performed with a solvent system consisting of 0.05% TFA in water (solvent A) and 60% CH_3CN in solvent A (solvent B), by applying a linear gradient from 100% to 20% solvent A in 47 min for BN (I) and from 100% to 50% solvent A in 47 min for BN (II). The flow rate was 4 mL/min, and the peptide peaks were detected with a UV detector at 220 nm. The new Rhenium$^{(V)}$ oxo complexes of the BN derivatives were characterized by ESI-MS and RP-HPLC.

Conjugation of ^{99m}Tc$^{(V)}$O-N$_3$S-BN Derivatives (Radioactive Complexes). Radiolabeling of the BN derivatives was performed by radioisotope exchange from a ^{99m}Tc$^{(V)}$O gluconate precursor, (sodium gluconate being used as an intermediate exchange ligand for ^{99m}Tc, with stannous chloride as the reducing agent) (*38*). Thus, a solid mixture containing 1 g of sodium gluconate ($C_6H_{11}NaO_7$), 2 g of sodium bicarbonate ($NaHCO_3$), and 15 mg of stannous chloride ($SnCl_2$) was homogenized and kept dry. Three milligrams of the above mixture was dissolved in 1 mL of a sodium pertechnetate solution ($Na^{99m}TcO_4$), containing 370−555 MBq (10−15 mCi) of ^{99m}Tc. An aliquot of 200 μL of the above solution was added to 100 μL of an aqueous solution (pH 1−2) containing 75 ng of each BN derivative. The mixture (pH 6−7) was homogenized by vortexing and allowed to react at 37 °C for 20 min.

Radiochemical Analysis. The labeling efficiency of the radiolabeled products was followed for up to 6 h postlabeling and determined by analytical RP-HPLC. Elution was performed with a solvent system consisting of 0.1% TFA in water (solvent A) and 0.1% TFA in methanol (solvent B), by applying the following gradient: from 0% to 80% solvent B (1−20 min), 80% solvent B (20−23 min), 80% to 0% solvent B (23−25 min), and 0% solvent B (25−30 min) at a flow rate of 1 mL/min. The eluent was passed through a UV detector at 220 nm and through a sodium iodide scintillation detector, both connected to a computer for data analysis and storage.

The ^{99m}Tc$^{(V)}$O gluconate precursor and radioactive BN derivatives were also analyzed by ITLC on Silica Gel (ITLC-SG) strips. Briefly, 5 μL of the reaction mixtures were applied on two different strips (13 cm × 1 cm) of SG paper (application point: 2 cm from the bottom). The radiochromatographs were developed in saline (0.9% NaCl) and methylethyketone (MEK), respectively, over a distance of 10 cm. After drying, the radioactivity of the strips was measured by electronic autoradiography. When normal saline was used, the radioactive complexes migrated with the solvent front, while using MEK they remained at the application point.

Lipophilicity: log *D* Values. To a solution containing 500 μL of *n*-octanol and 500 μL of phosphate-buffered saline (PBS, pH 7.4), 10 μL of each radiolabeled BN derivative was added. The resulting solution was vortexed and centrifuged at 810*g* at 4 °C for 10 min. An aliquot of both saline and octanol layers was collected, and the activity was measured in a γ-counter. The log *D* value was calculated as the log ratio of the radioactivity in the organic and aqueous phases (mean of three samples).

Cell Culture. Human androgen-independent prostate cancer cells (PC-3) were grown in DMEM Glutamax-I, supplemented with 10% (v/v) fetal bovine serum (FBS), 1% L-glutamine, and 1% penicillin/streptomycin. Cells were incubated in a controlled humidified atmosphere containing 5% CO_2 at 37 °C and were subcultured weekly after being detached from the flask surface by trypsin/EDTA solution (0.25%).

Metabolic Stability. *(I) Human Plasma and PC-3 Cell Culture.* The metabolic stability of the radiolabeled BN derivatives was studied in human plasma as well as in PC-3 cell culture. A blood sample from healthy donors in heparinized polypropylene tubes was immediately centrifuged at 2240*g* at 4 °C for 10 min, and the supernatant (plasma) was collected. One hundred microliters (3.7−7.4 MBq or 100−200 μCi) of each radiolabeled BN derivative was incubated with 900 μL of plasma at 37 °C. Fractions were withdrawn at 5, 15, 30, and 120 min, treated with ethanol (2:1 EtOH/aliquot, v/v) (*39*), centrifuged at 16 000*g* at 4 °C for 20 min, filtered through a Millipore GV (0.22 μm) filter, and analyzed by RP-HPLC as described above. *In vitro* degradation in cell culture was studied by incubation of 450 μL of a PC-3 cell suspension (2−2.5 × 10^6/mL) with 50 μL (3.7−7.4 MBq or 100−200 μCi) of each radiolabeled BN derivative at 37 °C. After incubation, fractions were withdrawn at 5, 15, and 30 min and treated with 1:1 acetonitrile/ethanol containing TFA (0.01%) (3:1 CH_3CN/EtOH/aliquot, v/v) (*10*). The mixture was centrifuged at 16 000*g* at 4 °C for 20 min, filtered, and analyzed by RP-HPLC.

(II) Kidney and Liver Homogenates. The metabolic stability was evaluated by incubation of each radiolabeled BN derivative in homogenized mouse liver and kidney samples at 37 °C. Liver

or kidneys were extracted from mice, rapidly rinsed with cold water, and immersed in 500 μL of chilled 50 mM Tris/0.2 M sucrose buffer, pH 7.4, where they were homogenized. Aliquots of 50 μL of each radiolabeled BN derivative (3.7−7.4 MBq or 100−200 μCi) were added to ca. 450 μL of tissue homogenates, containing the same amount of protein as this was determined by a colorimetric method using a BCA protein assay reagent (Pierce, Rockford, IL). Fractions withdrawn at 5 and 15 min were treated with ethanol (2:1 EtOH/aliquot, v/v) (*40*), centrifuged at 16 000*g* at 4 °C for 20 min, filtered through Millipore GV (0.22 μm) filter, and analyzed by RP-HPLC.

In Vitro Cell Binding Studies. The IC_{50} values of the new BN derivatives were assessed by a competitive cell binding assay utilizing [^{125}I-Tyr^4]BN as the GRPR specific radioligand and [Tyr^4]BN as a control compound. PC-3 cells suspended in a medium containing 1% FBS, 0.125% BSA, 0.25 mM PMSF, 1 μg/mL aprotinin, and 50 μg/L bacitracin were distributed in 24-well plates and incubated at 37 °C for 1 h in the presence of 25 000 cpm ^{125}I-[Tyr^4]BN (2200 Ci/mmol) and increasing concentrations of each BN derivative or its complex with nonradioactive $^{185/187}$Re, ranging from 10^{-12} to 10^{-6} M. In this assay, [Tyr^4]BN was used as the control peptide. After incubation, the cells were washed twice with cold wash buffer and lysed with 1 N NaOH. Radioactivity bound to the cells was counted in a γ-counter. IC_{50} values were calculated by nonlinear regression analysis, using the GraphPad Software (San Diego, CA, USA) Prism 4 computer fitting program. Experiments were carried out three times in duplicate.

Internalization and Efflux Analysis. For the *in vitro* internalization analyses, PC-3 cells were distributed in six-well plates (1−1.5 × 10^6 cells per well) at 37 °C in 5%CO_2/air atmosphere overnight in culture medium (DMEM with 10% FBS, L-glutamine, and 1% penicillin/streptomycin). On the day of the experiment, the medium was removed, and the cells were washed twice with cold wash buffer and were incubated in 1.2 mL of internalization medium (DMEM containing 1% FBS) in the presence of 100 000−300 000 cpm of each radiolabeled BN derivative (in 150 μL of 0.5% BSA/PBS buffer corresponding to ∼200 fmol of total peptide) at 37 °C for 5, 15, 30, 60, 90, and 120 min. Specificity of internalization was evaluated in the presence of 1 μM unlabeled native BN. Upon completion of the incubation, cells were washed twice with cold PBS to discard unbound peptide. Surface bound activity was removed by washing the cells twice for 5 min each time with an acid wash (50 mM glycine−HCl/0.1 M NaCl buffer, pH 2.8). The amount of internalized peptides was recovered by solubilizing the cells with 1 N NaOH at 37 °C. The internalized radioactivity (% of total added) was determined using a multisample γ-counter system.

Externalization studies of the maximum internalized radioactivity were also performed after a 30 min internalization period. The medium was discarded, and the cells were washed three times with cold buffer. New medium was added, and the cells were incubated at 37 °C. Sampling at 0, 15, 30, 60, and 90 min postinternalization was performed by an initial cold buffer wash of the cells, followed by acid wash (for removal of surface bound activity), as previously described, and finally by treatment with 1 N NaOH to extract the radioactivity remaining trapped. Results are expressed as the percentage of total bound activity for each time point. Internalized and remaining radioactivity were calculated as a function of time by using a Microsoft Excel program.

Biodistribution Analysis in Normal Swiss Mice. The *in vivo* behavior was studied in normal female Swiss mice (average weight 20 ± 2 g) by injecting 100 μL (50−75 ng/100 μL) (5.5 MBq or ∼0.15 mCi) of each radiolabeled BN derivative, diluted in saline (pH 7.0), via the tail vein. Animals were sacrificed at predetermined time intervals of 15, 30, 60, and 120 min postinjection (p.i.), and the main organs were removed, weighed, and counted, together with samples of blood, muscle, and urine, in a γ-counter system. In comparison to a standard of the injected solution, results were expressed as a percentage of the injected dose (%ID) per organ and per gram of each organ or tissue. For total blood radioactivity calculation, blood is assumed to be 7% of the total body weight. Receptor blocking studies were also carried out with coadministration of an excess amount (100 μL, 1 mg/mL) of native BN. Animals were sacrificed 30 min postinjection, and the tissues were removed, weighed, and counted as previously described. *In vivo* studies were performed in compliance with the European legislation for animal welfare. All animal protocols have been approved by the Hellenic Authorities.

Biodistribution Analysis in PC-3 Tumor Bearing SCID Mice. For the implantation of tumors, PC-3 cells freshly suspended in medium were subcutaneously injected in the left front flank at a concentration of 10^7 cells/animal. Tumors were allowed to grow for two to three weeks. Animals were fed with autoclaved rodent food and water *ad libitum* before and during the time of tumor growth. On the day of assay, the mice were injected via the tail vein with 100 μL of a solution of each radiolabeled BN derivative in saline, pH 7.0 (7.4 MBq or ∼0.2 mCi corresponding to 100−125 ng of total peptide), and were sacrificed at 30 and 60 min p.i. [BN (I)] and at 30, 60, and 120 min p.i. [BN (II)]. For the determination of nonspecific uptake, blocking experiments were performed, in which three mice received excess amounts of native BN (100 μL, 1 mg/mL) along with the radiolabeled BN derivatives and sacrificed at 30 min postinjection.

Dynamic γ-Camera Imaging. Evaluation of the novel SPECT radiolabeled BN derivatives was performed by dynamic imaging studies using a high resolution dedicated small animal γ-camera. Tumor-bearing mice were anaesthetized with 100 μL of 10% xylazine and 5% ketamine, 10 mg/kg mouse body weight prior to scanning, and positioned to the animal bed. One hundred microliters of approximately 7.4 MBq (∼0.2 mCi) of BN (II) was administered through the tail-vein prior to anesthesia. These imaging studies of 10 min per frame were performed up to 120 min p.i.

Statistical Analysis. All data are expressed as the mean of values ± standard deviation (mean ± SD). Data comparison was performed by using Student's *t*-test. $P < 0.05$ was considered significantly different.

RESULTS

Synthesis and Characterization. Synthesis of the two new BN derivatives was performed following an Fmoc-based SPPS protocol. The BN derivative without spacer [BN (I)] was obtained at a yield of about 40%. The introduction of the spacer Orn-Orn-Orn [BN (II)] led to a significant reduction in the yield. Thus, <10% of [BN (II)] was obtained. The chemical purity was higher than 95% for both derivatives, as determined by analytical RP-HPLC. Both derivatives were characterized with MS-ESI (Table 1).

Conjugation of $^{185/187}$Re$^{(V)}$O-N$_3$S-BN Derivatives (Nonradioactive Complexes). The nonradioactive complexes of the two new crude BN derivatives obtained after the exchange ligand reaction were purified by semipreparative RP-HPLC and characterized by analytical RP-HPLC and ESI-MS (Table 1). The retention times of the $^{185/187}$Re-$^{(V)}$ON$_3$S-BN derivatives, compared to those of the respective radioactive complexes, were similar after their co-injection into RP-HPLC, confirming that $^{185/187}$Re and ^{99m}Tc form complexes of similar structure (Table 2).

Table 1. Mass Spectra Analysis of the Pure BN Derivatives and of Their Complexes with Nonradioactive $^{185/187}$Re

N_3S-**X**-BN[2−14] derivative	molecular mass (calcd.) (Da)	molecular mass (found) (Da)
(I)	1725.9	1725.8 (*m/z*: 863.9, $[M + 2H]^{2+}$)
(II)	2068.4	2068.8 (*m/z*: 690.6, 1035.4 $[M + 3H]^{3+}$, $[M + 2H]^{2+}$)
$^{185/187}Re^{(V)}ON_3S$-**X**-BN[2−14] derivative	molecular mass (calcd.) (Da)	molecular mass (found) (Da)
(I)	1924.9	1925.6 (*m/z*: 963.8, $[M + 2H]^{2+}$)
(II)	2267.6	2268.0 (*m/z*: 757.0, 1135.0 $[M + 3H]^{3+}$, $[M + 2H]^{2+}$)

Table 2. Analytical Data of N_3S-X-BN[2−14] and log $D_{(O/W)}$ for Their ^{99m}Tc Derivatives[a]

$^{185/187}Re^{(V)}ON_3S$-**X**-BN[2−14] derivative	R_T[b] (min)	$^{99m}Tc^{(V)}ON_3S$-**X**-BN[2−14] derivative	R_T[b] (min)	log $D_{(o/w)}$[c] ± SD
(I)	15.8	(I)	16.1	-1.60 ± 0.03[d]
(II)	13.9	(II)	14.2	-1.72 ± 0.03[d]

[a] Elution system: flow 1 mL/min; A, 0.1% TFA/H_20; B, 0.1% TFA/MeOH. [b] R_T: retention time. [c] log $D_{(o/w)}$ partition coefficient between *n*-octanol and PBS (pH 7.4). [d] Significant differences ($p < 0.05$) between BN derivatives (I) and (II).

Radiolabeling−Radiochemical Analysis. Radiolabeling of the two new BN derivatives with ^{99m}Tc was performed by the preconjugation approach using the $Tc^{(V)}O$ gluconate precursor as an intermediate exchange ligand. A two-strip ITLC-SG method for the analysis of a precursor showed that no amount of either pertechnetate $^{99m}TcO_4$ or of colloidal ^{99m}Tc was present. The radiochemical yield for both BN derivatives was higher than 98%, providing a single radioactive species, as detected by both RP-HPLC and paper chromatography (ITLC-SG). The stability of the new derivatives, tested up to 6.0 h postlabeling, remained high (>90%). The RP-HPLC retention time of BN (I) was 16.1 min, whereas that of BN (II) was lower, 14.2 min, indicative of its higher hydrophilic nature (Table 2). The lipophilicity of the two radiolabeled BN derivatives under study was evaluated by determining the log *D* partition coefficient values between *n*-octanol to PBS, at pH 7.4 (Table 2).

Metabolic Stability. *(I) Human Plasma and PC-3 Cell Culture.* The rate of catabolism of both new ^{99m}Tc-labeled BN derivatives was higher in cell culture than in human plasma. After 120 min of incubation, the radiolabeled BN derivatives remained intact in human plasma at a percentage of 60%. After 30 min of incubation with PC-3 cells, ∼30% of the radioactivity corresponded to the intact BN (I), while ∼50% of BN derivative (II) was found still intact at the same time period. Thus, the spacer group Orn-Orn-Orn did not greatly affect plasma stability, while it slightly increased cell stability.

(II) Kidney and Liver Homogenates. Enzymatic degradation tested in kidney and liver homogenates was found to occur after just 5 min of incubation. Thus, in kidney homogenates, BN derivatives (I) and (II) remained intact >40% and >45%, respectively, the rest being metabolized to more hydrophilic species of lower retention times. Further incubation for 15 min led to a percentage of 20−30% intact peptide for both BN derivatives. Catabolism in liver was much faster in the case of BN (I), which, within 5 min of incubation, was almost totally degraded, while degradation rates of BN (II) were found to be substantially slower (Figure 2).

In Vitro Cell Binding Studies. The binding affinity of N_3S-X-BN[2−14] and of their $^{185/187}$Re complexes for the GRPR was evaluated in the human prostate adenocarcinoma cell line PC-3. A typical sigmoid curve for displacement of ^{125}I-[Tyr^4]BN from PC-3 cells as a function of increasing concentration of all five different cold ligands used was obtained. The determined IC_{50} values are summarized in Table 3. BN derivative (I) (with or without Re) was less efficient in inhibiting the binding of ^{125}I-[Tyr^4]BN on PC-3 cells than [Tyr^4]BN (control). BN (II) (free of or complexed with Re) showed better affinity than BN (I).

Internalization and Efflux Analysis. The grade of uptake (internalization) and efflux (externalization) as a function of time of the two radiolabeled BN derivatives under study was assessed in human cancer PC-3 cells at 37 °C, in the presence (blocking experiments) or absence of native BN. Figure 3 reports the results of this study. Within the first 30 min of incubation, the proportion of radioactivity migrating into the cells increased significantly and remained at this level for 2 h.

More specifically, relative to the cell-associated activity after 5 min of incubation, 34% of BN (I) and 66% of BN (II) were internalized, attaining a value of 78% and 88% after 120 min, respectively. Although the membrane-bound activity was rather similar between the two radiolabeled BN derivatives, the internalized activity related to the total added substantially differed from one derivative to the other with the value for BN (II) being almost 5-fold higher than that for BN (I) (Figure 3A). To evaluate the externalization of ^{99m}Tc-conjugates from PC-3 cells after 30 min of incubation, cells were washed with acid wash buffer, for removal of surface-bound activity and then were further incubated in the medium. Measurements up to 90 min postincubation showed that around 53% of BN (I) and 63% of BN (II) remained trapped in the cells (Figure 3B).

Biodistribution Analysis in Normal Swiss Mice. Comparative *in vivo* studies in physiological experimental models at 15, 30, 60, and 120 min postinjection for both studied derivatives are summarized in Figure 4. Both ^{99m}Tc-Bombesin derivatives demonstrated fast blood clearance with the blood levels of BN (II) [0.51 ± 0.06 and 0.16 ± 0.06 (%)ID/g)] being lower than those of the BN (I) [1.00 ± 0.17 and 0.46 ± 0.05 (%)ID/g)], at 60 and 120 min p.i., respectively. Statistical evaluation (*t*-test) of the data sets of the two studied BN derivatives at 60 and 120 min demonstrated *p*-values <0.01 and <0.001. No significant uptake or retention in the stomach was observed, indicating that there is minimal, if any, release of free $^{99m}TcO_4^-$ derived from *in vivo* degradation of ^{99m}Tc of the N_3S complex. Liver activity values were relatively low, compared to the activity accumulated at the other normal tissues and seem to correlate with the log *D* values (Table 2). Similar to that in the liver, intestinal uptake was relatively low. The predominant excretion route for both studied derivatives was via the kidneys to urine. The higher kidney retention found for BN (II) is attributed to the increase of the overall positive charge of this derivative due to the presence of ornithine. The GRPR-positive pancreas also showed high uptake, significantly inhibited by the coadministration of an excess amount of blocking agent, while for BN (II), accumulation was significantly higher [27.89 ± 7.78, 16.72 ± 3.57, and 10.26 ± 1.64 (%)ID/g] at 15, 30, and 60 min p.i. as compared to [13.38 ± 3.99, 9.49 ± 3.31, and 5.20 ± 3.88 (%)ID/g] of BN (I). Statistical evaluation (*t*-test) of the data sets of the two studied BN derivatives at 15, 30, and 60 min demonstrated *p*-values <0.05.

Biodistribution Analysis in PC-3 Tumor-Bearing SCID Mice. Both ^{99m}Tc-bombesin derivatives were further tested *in vivo* in PC-3 tumor-bearing mice. The results are presented in Table 4. Tumor sizes in this study varied from 0.1 to 0.5 g. The greater portion of the ^{99m}Tc-Bombesin derivatives cleared efficiently from the bloodstream within 60 min p.i., with blood values being 0.52 ± 0.05 and 1.07 ± 0.12 (%)ID/g for radiolabeled BN (I) and BN (II) derivatives, respectively. They were mainly excreted into the urine via the kidneys. Both BN (I) and BN (II) were capable of rapidly targeting the GRP

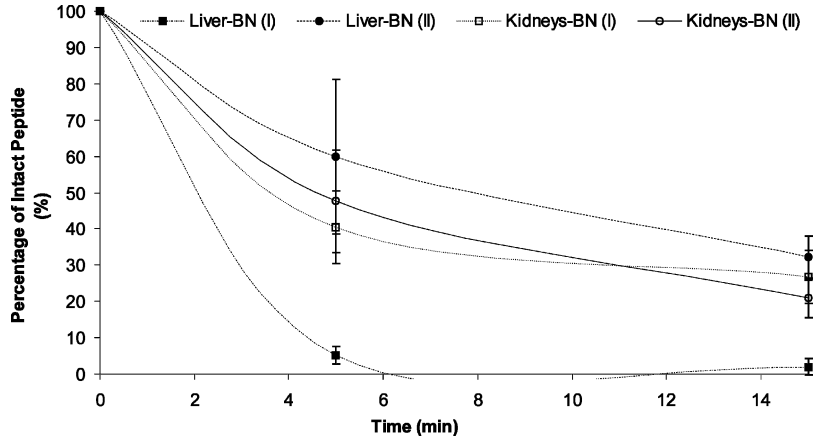

Figure 2. Degradation study of the two new $^{99m}Tc^{(V)}ON_3S$-**X**-BN[2−14] derivatives after incubation at 37 °C in liver [BN (I), ■; BN (II), ●] and kidney [BN (I), □; BN (II), ○] homogenates. Vertical bars indicate standard deviation (SD). Results are expressed as the mean of 3−5 experiments ± SD.

Table 3. IC_{50} Values of N_3S-X-BN[2−14] Derivatives and of Their Complexes with $^{185/187}Re$ Obtained by Displacement of ^{125}I-[Tyr^4]BN from PC-3 Cells

compound	IC_{50} ± SD
Tyr^4-BN (control)	1.6 ± 0.3
N_3S-X-BN[2−14] Derivatives	
(I)	3.2 ± 0.6
(II)	1.5 ± 0.2
$^{185/187}Re^{(V)}ON_3S$-**X**-BN[2−14] Derivatives	
(I)	3.0 ± 0.7
(II)	2.2 ± 0.1

receptor positive tissues, that is, the pancreas as well as the PC-3 tumor, within 30 min p.i. [(11.08 ± 2.76, 4.56 ± 0.95) (%)ID/g for BN (I) and (11.07 ± 4.2, 5.23 ± 2.10) (%)ID/g for BN (II)]. Specificity of *in vivo* delivery of the two novel BN derivatives was demonstrated with blocking by coadministration of an excess amount of the nonradiolabeled native BN at 30 min p.i.. In this case, uptake in the pancreas and PC-3 tumor was found to be significantly reduced ($p < 0.05$). Comparative studies between the radiolabeled derivatives BN (I) and BN (II) at 60 min p.i., indicated distinct differences in the uptake in both receptor-rich organs. In particular, BN (I) showed a significant reduction of accumulation in the tumor (1.02 ± 0.18%ID/g) and pancreas (4.17 ± 0.99%ID/g) related to 30 min p.i. BN (II) showed a more favorable, statistically different biodistribution ($p < 0.01$), in the tumor (7.14 ± 0.87%ID/g) and pancreas (27.59 ± 6.86%ID/g) than BN (I). Tumor-to-nontarget ratios of BN (II) were also significantly higher than those of BN (I) for the organs and tissues examined (blood, muscles, liver, and kidneys) ($p < 0.05$) at 60 min p.i. Tumor retention of BN (II) was also observed at 120 min p.i. (7.92 ± 0.79%ID/g) demonstrating even higher tumor/blood ratios than that for 60 min p.i. ($p < 0.05$). Moreover, intestinal uptake of BN (II) reached a maximum at 120 min p.i. (6.75 ± 0.91%ID/g) while liver accumulation was relatively low at the same time point (2.62 ± 0.17%ID/g).

Dynamic γ-Camera Imaging. The localization of ^{99m}Tc-labeled BN (II) in PC-3 tumor-bearing mice exhibited considerably higher tumor uptake than radiolabeled BN (I). This was further evaluated by γ-ray scintigraphy. The PC-3 tumor at the right front flank was visible with clear contrast from the adjacent background as early as 10 min after injection and remained observable up to 120 min p.i. Prominent uptake was also observed in the kidneys. Clearance of the radioactivity through the urinary bladder was evident as well (Figure 5). In contrast, the same tumor was not visualized in another SCID mouse, which had received a high dose of native BN along with the radiolabeled BN (II) derivative (Figure 6).

DISCUSSION

Much attention has been recently focused on radiolabeled BN-like peptides with different types of metal chelators, peptide sequences, and spacer groups (*9, 41*). As far as the spacer attaching the ^{99m}Tc-chelating moiety onto the peptide is concerned, this may be just an inactive moiety not affecting the properties of the parent molecule, but it may also be a pharmacokinetic modifier, able to improve stability, binding affinity, internalization into the tumor cells and biodistribution (*42*). Suitable spacer groups include peptides (amino acids linked together) alone (*18−22*), nonpeptide groups (for example a hydrocarbon chain from 3 to 9 carbon atoms) (*16, 24, 34, 35*) or a combination of an aminoacid sequence and a nonpeptide spacer (*17, 23, 25, 32*).

In the framework of the present study, the new BN derivatives were prepared by the well-established technique of solid-phase peptide synthesis (SPPS). The radiolabeling of BN derivatives was accomplished by a transchelation reaction. Prior to reaction with the selected amino acid chelator, Gly-Gly-Cys, ^{99m}Tc was reduced and complexed with the labile gluconate ligand. Nonradioactive $^{185/187}Re$ complexes of the BN derivatives, used for structural characterization, were prepared by the same method, as Re and Tc are both elements of the VIIB row of the periodic table and display the same complexation chemistry. The claim that $^{185/187}Re$- and ^{99m}Tc-BN derivatives have the same structure was verified by their similar retention times after their co-injection in a RP-HPLC column. The radiolabeled BN derivatives (I) and (II) were easily obtained in a yield higher than 98%. These results are consistent with previous studies, which demonstrated that N_3S ligand systems form stable peptide conjugates, obtained in high yield and high specific activity by transchelation from rhenium or technetium (V) gluconate precursors (*16, 31*).

Stability assays were performed in order to evaluate whether spacer modifications were sufficient for maintaining the stability of the ^{99m}Tc-BN derivatives (I) and (II) *in vivo* to ensure efficient delivery of radioactivity at the target. The stability of these new BN derivatives was determined *in vitro* in human plasma, human prostate cancer PC-3 cells, and in liver and kidney homogenates. After incubation at 37 °C, a higher stability was observed in plasma, where both derivatives remained intact at a level of 60% after 120 min. It is worthwhile to mention that during the first crucial 15 min of incubation the percentage of intact BN (I) and (II) was about 80 and 70%, respectively. In contrast,

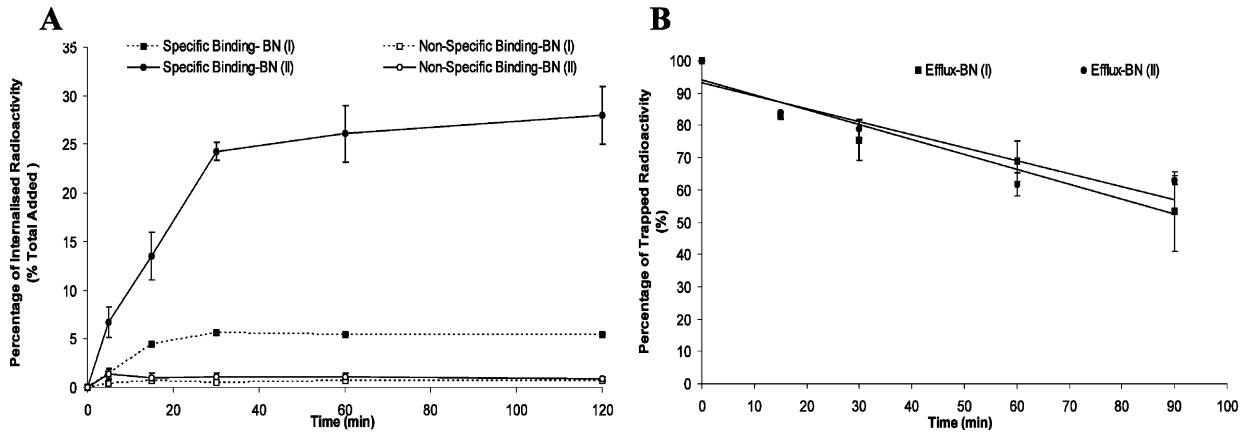

Figure 3. Internalization (A) and externalization (B) after maximum internalization (30 min of incubation at 37 °C) of the two $^{99m}Tc^{(V)}ON_3S$-**X**-BN[2−14] derivatives. Data represent the percentage of internalized and trapped radioactivity into the cells, in relation to the totally added radioactivity [BN (I), ■; BN (II), ●]. Vertical bars indicate standard deviation (SD). Results represent the mean of 2−3 experiments ± SD, each performed in triplicate.

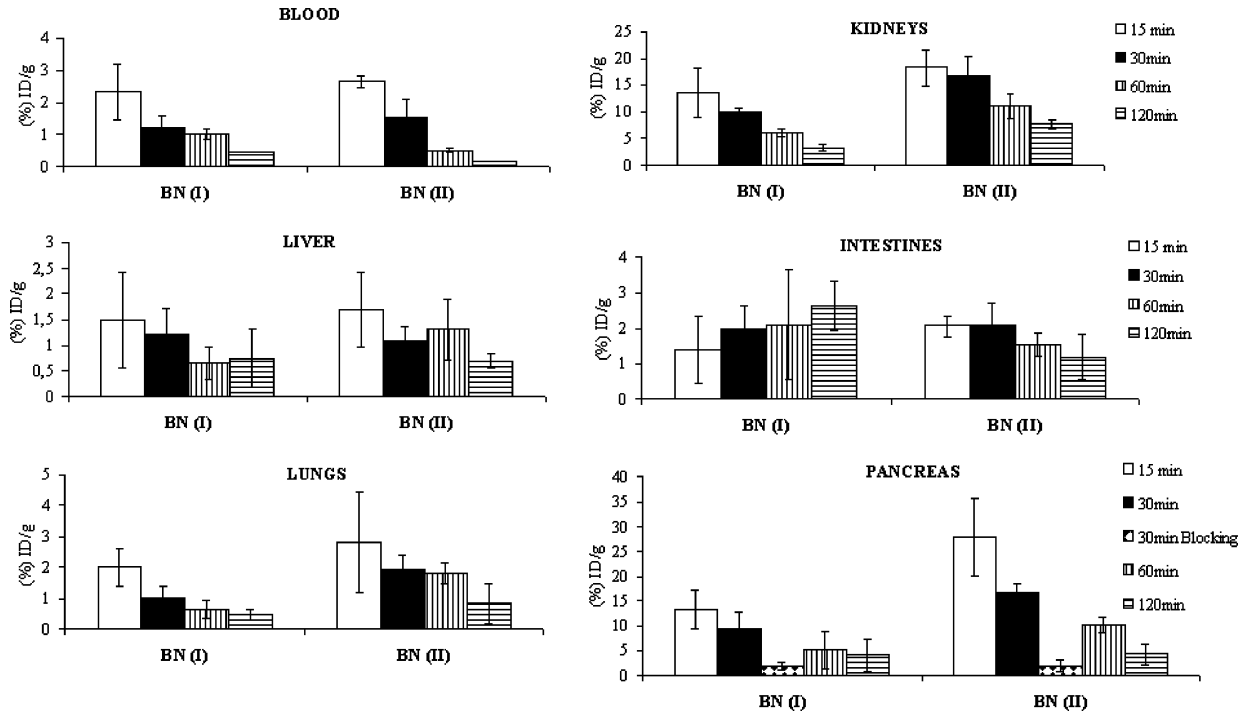

Figure 4. Comparative study of tissue or organ uptake for the two new $^{99m}Tc^{(V)}ON_3S$-X-BN[2−14] derivatives in normal Swiss mice at the time intervals of 15, 30, 60, and 120 min. Biodistribution values represent the mean ± standard deviation of %ID/g (3−5 animals were used per time point). Blocking studies were performed by coinjection of 3 animals with excess amounts of native BN.

the degradation was much faster in PC-3 cells, being more prominent for BN (I) than for BN (II). Nevertheless, a rapid catabolism in tumor cells would not necessarily be a problem, if the peptide is quickly internalized, and the metabolic products remain trapped inside the cell (*13*). However, even lower stability was found in liver and kidney homogenates with various metabolites of lower R_T values being formed, but in all cases, nondetectable technetium traces were released from the breakdown of the amino acid chelator ^{99m}Tc-Gly-Gly-Cys. Overall, results obtained during the metabolic stability study demonstrated that the insertion of the spacer group Orn-Orn-Orn seems to stabilize the resulting derivative (II) in cell culture and keep it more stable during exposure to the proteolytic action of liver enzymes. This is possibly due to the presence of the 3 nonnatural amino acids, which are not so easily recognized by the proteolytic liver enzymes.

The binding affinity of BN (I) and (II) for GRP receptors was in the nanomolar range, comparable to that of [Tyr^4]-BN and to those reported for Triaza-X-BBN (7−14) (X = SSS, GSG, GGG, and b-Ala) (*18*) and $Re(H_2O)(CO)_3$-Dpr-X-BBN (X = NNN, NNN-βAla, and NNN-5Ava) (*43*). The highest affinity among the tested BN derivatives was observed in the case of BN (II), while its complex with $^{185/187}$Re had the second better binding affinity for the GRPR. Once the radioactive BN derivative is residualized within cancer cells upon binding on the cell surface of GRPRs, then a specific delivery of diagnostic/therapeutic dose occurs. Experiments designed to determine the fraction of both studied ^{99m}Tc-derivatives internalized within the PC-3 cells showed that there were significant differences in the amount internalized for each of them at all time points. BN (II) showed a much higher degree and rate of internalization than BN (I). Even if the IC_{50} values of the unlabeled derivatives are similar, the internalization level of ^{99m}Tc-BN (I) is lower than ^{99m}Tc-BN (II). This discrepancy could be explained by the presence of the hydrophilic linker of Orn-Orn-Orn that leads to a final conformation of the whole complex of radioconjugate−

Table 4. Biodistribution Data of Radiolabeled BN (I) and (II) Derivatives in Female SCID Mice Bearing PC-3 Tumors[a]

	BN (I) derivative			BN (II) derivative	
organ/tissue	30 min ± SD	60 min ± SD	30 min ± SD	60 min ± SD	120 min ± SD
blood	2.57 ± 1.59	0.52 ± 0.05	3.33 ± 0.15	1.07 ± 0.12	0.24 ± 0.05
heart	1.86 ± 1.83	0.24 ± 0.01	1.45 ± 0.12	0.53 ± 0.05	0.42 ± 0.24
lung	2.23 ± 0.67	0.46 ± 0.08	2.40 ± 0.33	2.02 ± 0.83	1.39 ± 0.48
liver	2.81 ± 1.70	1.54 ± 0.08	1.57 ± 0.12	2.46 ± 0.63	2.62 ± 0.17
spleen	2.23 ± 1.39	0.64 ± 0.51	1.32 ± 0.06	1.06 ± 0.30	0.65 ± 0.36
stomach	1.86 ± 0.09	0.57 ± 0.04	0.46 ± 0.01	0.83 ± 0.80	2.61 ± 0.42
intestines	2.08 ± 1.55	1.74 ± 0.57	1.21 ± 0.41	2.69 ± 0.43	6.75 ± 0.91
kidneys	16.50 ± 1.42	5.56 ± 0.52	10.11 ± 2.78	25.49 ± 1.61	16.18 ± 2.17
pancreas	11.08 ± 2.76†	4.17 ± 0.99	11.07 ± 4.2*	27.59 ± 6.86	25.35 ± 5.95
blocked pancreas[b,c]	1.69 ± 1.42†	ND[d]	1.84 ± 0.22*	ND[d]	ND[d]
muscles	1.04 ± 0.91	0.11 ± 0.00	0.82 ± 0.14	0.51 ± 0.35	0.51 ± 0.38
PC3 tumor	4.56 ± 0.95§	1.02 ± 0.18	5.23 ± 2.10**	7.14 ± 0.87	7.92 ± 0.79
blocked tumor[b,c]	0.91 ± 0.60§	ND[d]	0.86 ± 0.17**	ND[d]	ND[d]
tumor to blood	1.77	1.96	1.57	6.67	33.32
tumor to muscles	4.38	9.27	6.38	14.00	15.53
tumor to liver	1.62	0.66	3.33	2.90	3.02
tumor to kidney	0.28	0.18	0.52	0.28	0.49

[a] Results are expressed as the mean ± standard deviation of %ID/g (3 animals were used per time point). [b] Blocking study was performed by co-injecting 3 animals with an excess amount of native BN along with the radiolabeled BN derivative. [c] Statistical analysis with †,§p values and *,**$p <$ 0.05 being considered significantly different versus unblocked. [d] ND = not determined.

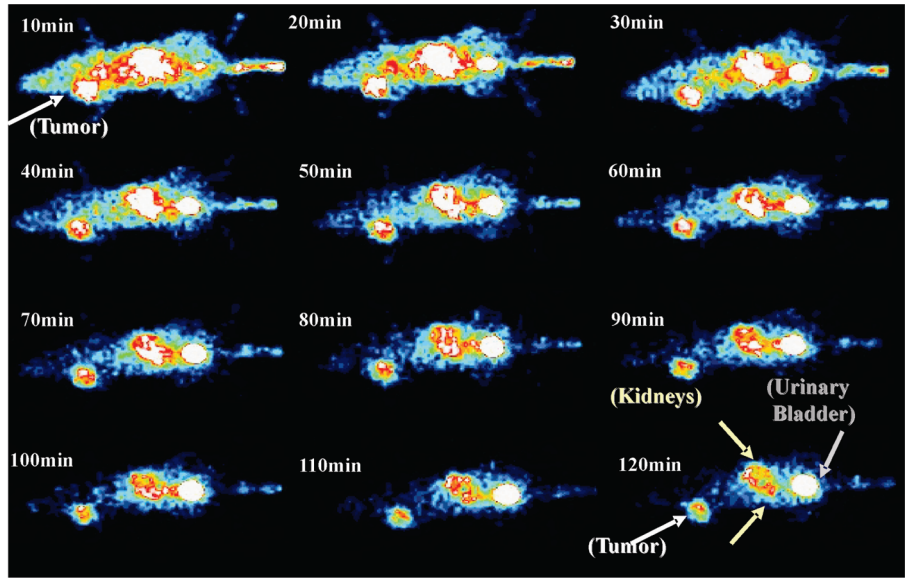

Figure 5. Gamma-ray dynamic images of 10 min per frame up to 120 min of a tumor bearing mouse for radiolabeled BN derivative (II). Arrows in white, yellow, and gray indicate the presence of the tumor, kidneys, and urinary bladder, respectively.

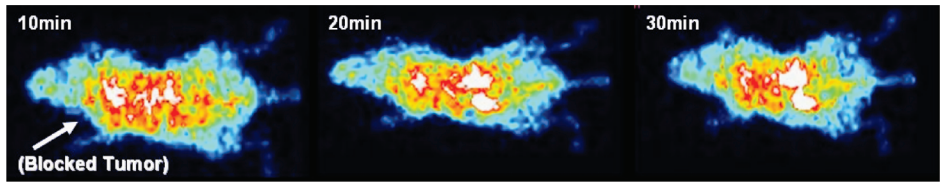

Figure 6. Gamma-ray dynamic images of 10 min per frame up to 30 min of a blocked tumor bearing mouse (PC-3 onto the right front flank) for radiolabeled BN (II). The arrow (in white) indicates the presence of the blocked tumor.

receptor, which probably induces penetration into the cells. This high level of internalization of BN (II) explains in part its superior *in vivo* properties compared to those of BN (I). Efflux studies indicated that the BN derivatives were rather rapidly released from PC-3 cells. Thus, about a half-for BN (I) and less than a half-for BN (II) of the internalized radioactivity was released in the first 90 min, probably due to the ability of functional intracellular proteases to degrade them. The rate of residualization of radioactivity inside cells is in accordance with other reports (*16, 17*). In view of the design of radiolabeled BN peptides for therapy, new analogues should be developed with higher retention time into the cells.

An ideal pattern of biodistribution is one in which any radioactivity not bound to the receptive positive organ receptors or tumor is rapidly cleared from the blood and efficiently excreted without retention in any normal organ (*9, 42*). In fact, during biodistribution studies in healthy mice, uptake in the pancreas of the derivative (II) from 15 to 60 min p.i. was higher than that of derivative (I). Clearance of radioactivity from the pancreas with time is probably due to excessive enzymatic

activity in this organ. Similar behavior has been reported for other ^{99m}Tc-labeled BN analogues such as ^{99m}Tc-Demobesin I (*39*) and [^{99m}Tc−P_2S_2]BN(7−14) (*44*). Specificity of the novel radiolabeled BN derivatives for the GRPR-rich healthy positive tissues (such as the pancreas) was confirmed by *in vivo* blocking after coadministration of native BN. The main clearance route of radioactivity for both derivatives was via the kidneys to urine. Although the changes in the linker sequence had a considerable effect on the reduction of liver accumulation, kidney values remained high enough, 7.73 ± 0.90% I.D./g, at 120 min p.i. for BN(II), while for the BN (I) derivative, they were 3.24 ± 0.57% I.D./g since more positively charged compounds are known to accumulate in the kidneys (*22*). However, an entirely renal route of excretion is preferable to a partly hepatobiliary clearance (*45*). Nonetheless, for prostate cancer radioimaging, there is high demand for achieving minimal accumulation of radioactivity in the abdominal area (intestines, stomach, liver, kidneys, and bladder). Thus, decreasing the lipophilicity of the radiolabeled BN derivatives serves to increase renal/urinary excretion, which is not preferable for detecting prostate tumors. Minimization of bladder interference can be achieved by several strategies such as differential timing of the images so as to highlight prostate gland and bladder drainage by means of an indwelling tube (*46*). In clinical practice, patients are asked to void the bladder before scintigraphy.

Results from the *in vivo* investigation in SCID mice, presented in Table 4 for BN (I) and (II), showed distinct differences in the biodistribution pattern of the two compounds in both receptor-positive and nontarget organs. Nevertheless, at the early time point of 30 min p.i., BN (I) showed tumor and pancreas uptake (4.56 ± 0.95 and 11.08 ± 2.76% I.D./g) values comparable to the corresponding values of BN (II) (5.23 ± 2.10 and 11.07 ± 4.2% I.D./g). The activity accumulated within the receptor-rich organs was quickly washed out at 60 min p.i. (1.02 ± 0.18 and 4.17 ± 0.99% I.D./g) for BN (I). However, a significant uptake of BN (II) in the GRPR-bearing tumor and pancreas was observed at 60 and 120 min p.i.. The greater accumulation of BN (II) in the pancreas may be explained by the higher receptor densities in this tissue in relation to the tumor and by the better penetration in the pancreatic acini cells in comparison to the weak vasculatory architecture of the PC-3 tumor (*47*). Receptor-bearing tissues, such as the tumor and pancreas present a relatively high uptake 30 to 60min p.i., with values remaining high up to 120 min p.i.. Pancreatic retention for BN (II) in SCID mice compared to that in normal mice is not fully understood. However, similar differences in the values of the pancreas concerning healthy animals and those with tumors have also been observed in a recent report by Faintuch et al., which compares ^{99m}Tc-HYNIC-BN with ^{99m}TcN(PNP6)-Cys-BN, and have been attributed to the different animal models used (*46*). Moreover, the washout of BN (II) from the PC-3 tumor is slow unlike its rate of externalization from PC-3 cells. This discrepancy may be due to the fact that the higher polarity of BN (II) probably favors pancreas and tumor penetration and retention (*48*). However, it should also be taken into consideration that the human tumor-bearing models are supported by murine vasculature architecture (*49*). It seems that the approach of using normal mice as a screening tool for GRPR targeted radiopharmaceuticals may be inadequate for predicting *in vivo* uptake in GRPR positive tumors (*25*). Furthermore, tumor to background ratios that are quite high at 60 min p.i. increased or remained constant at 120 min p.i. in the case of blood and muscles, respectively, illustrating a very good profile of BN (II) for GRPR targeted applications. GRPR specificity was confirmed by the receptor-blocking study at 30 min p.i. where the inhibition of uptake in these tissues was effective for both derivatives, by co-injection with a high dose of native bombesin. Similar trends were also observed for the other BN receptor positive organs, such as the intestines, where uptake of the radiolabeled BN derivatives was significantly reduced by coadministration of native bombesin (data not shown). It is also important to notice, as has already been mentioned in the case of healthy mice, that these modifications performed at the spacer site led to nonsignificant hepatic uptake and that the main clearance route of ^{99m}Tc radioactivity from the SCID mice is via the renal system. Nevertheless, the structure of spacer Orn-Orn-Orn did have an important effect on the retention of radioactivity in the kidneys of SCID mice, which was higher relative to what was observed with normal mice as also referred to by others (*25*). Obviously, this persistent kidney retention that the BN (II) derivative demonstrated is not optimal and is higher than that of BN (I). But as BN (II) has shown among the highest tumor and pancreas targeting efficacy of the ^{99m}Tc-BN conjugates of this type, following the Tc-labeled BN derivatives reported by Nock et al. (*39*) and Cescato et al. (*50*), this can be a problem only in the application of this compound for therapy due to potential nephrotoxicity (*25, 51*). To our knowledge, it may be possible to accelerate the wash out of BN (II) from kidneys by coadministration of polyornithine (more than 5 chain length), an approach that has been suggested in a previous report by Behe et al. (*52*), where uptake of ^{111}In-DTPA-DGlu^1-minigastrin in the kidneys was blocked by the use of polyglutamic acids.

A direct comparison of the tumor uptake observed for BN (I) and (II) with other publications using ^{99m}Tc-labeled bombesin derivatives is somehow difficult since in most of the reports, the C-terminal amidated BN(7−14) sequence or other stabilized forms of it were studied, while in the present study, the whole bombesin sequence is used. The full length sequence was proved by Gourni et al. (*35*) to lead to practically exclusive renal elimination. Radiochemical investigations of ^{99m}Tc(H_2O)(CO_3)-Dpr-SSS-BN(7−14) in PC-3 tumor-bearing mice by Smith et al. showed that tumor uptake was higher at 1 h p.i. (3.68 ± 0.92% I.D./g) than BN (I) and lower than BN (II) (*14*). The same group has also studied the pharmacokinetic properties of ^{99m}Tc(H_2O)(CO_3)-Dpr-NNN-βAla-BN(7−14) in PC-3 tumor-bearing mice, where two tumors were developed on the bilateral flank with accumulations of 2.79 ± 0.95% I.D./g and 3.28 ± 1.18% I.D./g at 1 h. p.i (*43*). Tumor uptake and retention were lower compared to ^{99m}Tc(H_2O)(CO_3)-Dpr-SSS-BN(7−14), which also seemed to be superior to ^{99m}Tc(H_2O)(CO_3)-Dpr-NNN-βAla-BN(7−14) for imaging prostate tumors. Results from the *in vivo* evaluation of ^{99m}Tc(CO_3)-pyrazolyl-X-BN(7−14) in SCID mice bearing xenografted human prostate PC-3 tumors by S. Alves et al. showed that maximum tumor uptake (1.76 ± 0.79% I.D./g and 1.76 ± 1.20% I.D./g) at 1 h p.i. for SSS and GGG linkers was higher when compared to that of BN (I) and lower than that of BN (II) (*16*). In a recent study with ^{99m}Tc(I)-BN derivatives consisting of different neutral or charged polar linkers (*53*), it was shown that by introducing a single negative charge in the form of β^3hGlu, the *in vivo* profile was improved exhibiting higher tumor uptake and retention. This general concept of inserting polar rather than lipophilic linkers, between the chelator and the binding sequence and ameliorating in this way the biodistribution pattern (higher tumor uptake and retention), has also been supported by our results as well as by a recent study of Garayoa et al. with ^{99m}Tc$(CO)_3$-glycated-BN derivatives (*48*). More specifically, ^{99m}Tc(I)-Ala(^{N}TG)-βAla-βAla-(Cha^{13}, Nle^{14})-BN(7−14) exhibited accumulation similar to that of BN (II) and higher than that of BN (I) at 30 min p.i. and a notable tumor localization at further studied time points.

The scintigraphic dynamic images obtained in SCID mice bearing human PC-prostate cancer tumors demonstrated an easy delineation of the neoplastic region by the BN (II) derivative

up to 120 min p.i.. At the same time, low background accumulation was observed, which is consistent with the biodistribution data and the tumor/tissue ratios reported.

CONCLUSIONS

Significant progress has been made over the past years in the development of new radiolabeled candidates for targeting peptide receptors, by separation of the radiolabeling area from the receptor-targeting peptide moiety. The structural tuning introduced in the N_3S-BN[2−14] derivatives, via the concept of modifications at the spacer site is very promising in order to visualize GRP receptors expressed at cell membranes of various tissues. Using Orn-Orn-Orn as a spacer compared to no spacer at all resulted in higher stability and greater internalization of the ^{99m}Tc-labeled species in cells, in a considerably better uptake in target-specific pancreatic and tumor tissue and finally in high-quality SPECT images. From previous studies, it is generally accepted that high and persistent localization of radioactivity in kidneys is caused by long residence times of radiometabolites generated after lysosomal degradation, following glomerular filtration and subsequent reabsorption into renal cells (*54*). On the basis of these findings, efforts are being made to inhibit tubular reabsorption of radiolabeled peptides by competitive blockage (*52*), charge modification with amino acid substitutions (*10, 11, 55*), and PEGylation (*22, 56*). More wide-ranging modifications of the spacer are necessary to promote an efficient excretion of ^{99m}Tc-BN based radiopharmaceuticals of this type without significant retention in any normal organs such as the kidneys.

ACKNOWLEDGMENT

We thank Dr. Leondios Leondiadis for ESI-MS analyses performed at the Mass Spectrometry and Dioxin Analysis Lab, NCSR "Demokritos". The present work has been financially supported by the General Secretariat for Research and Technology.

LITERATURE CITED

(1) Anastasi, A., Erspamer, V., and Nucci, M. (1972) Isolation and aminoacid sequences of alytensin and bombesin, two analogous active tetradecapeptides from the skin of european discoglossid frogs. *Arch. Biochem. Biophys. 148*, 443–446.

(2) Nagalla, S. R., Barry, B. J., Falicks, A. M., Gibson, B. W., Taylor, J. E., Dong, J. Z., and Spindel, E. R. (1996) There are three distinct forms of bombesin. *J. Biol. Chem. 271*, 7731–7737.

(3) Ohki-Hamazaki, H., Iwabuchi, M., and Maekawa, F. (2005) Development and function of bombesin-like peptides and their receptors. *Int. J. Dev. Biol. 49*, 293–300.

(4) Cornelio, D. B., Roesler, R., and Schwartsmann, G. (2007) Gastrin-releasing peptide receptor as a molecule target in experimental anticancer therapy. *Ann. Oncol. 18*, 1457–1466.

(5) Dietrich, J. B. (1994) Neuropeptides, antagonists and cell proliferation: bombesin as an example. *Cell. Mol. Biol. 40*, 731–746.

(6) Patel, O., Shulkes, A., and Baldwin, G. S. (2006) Gastrin-releasing peptide and cancer. *Biochim. Biophys. Acta 1766*, 23–41.

(7) Qu, X., Xiao, D., and Weber, C. H. (2003) Biologic relevance of mammalian bombesin-like peptides and their receptors in human malignancies. *Curr. Opin. Endocrinol. Diabetes Obes. 10*, 60–71.

(8) Giblin, M. F., Veerendra, B., and Smith, C. J. (2005) Radiometallation of receptor-specific peptides for diagnosis and treatment of human cancer. *In Vivo 19*, 9–29.

(9) Smith, C. J., Volkert, W. A., and Hoffman, T. J. (2005) Radiolabeled peptide conjugates for targeting of the bombesin receptor superfamily subtypes. *Nucl. Med. Biol. 32*, 733–740.

(10) Garayoa, G. E., Ruegg, D., Blauenstein, P., Zwimpfer, M., Khan, I. A., Maes, V., Blanc, A., Beck-Sickinger, A., Tourwe, A. G., and Schubiger, P. A. (2007) Chemical and biological characterization of new $Re(CO)_3$/99m$Tc(CO)_3$ bombesin analogues. *Nucl. Med. Biol. 34*, 17–28.

(11) Garayoa, E. G., Schweinsberg, C., Maes, V., Ruegg, D., Blanc, A., Blauenstein, P., Tourwe, D. A., Beck-Sickinger, A. G., and Schubiger, P. A. (2007) New [^{99m}Tc]bombesin analogues with improved biodistribution for targeting gastrin releasing-peptide receptor-positive tumors. *Q. J. Nucl. Med. Mol. Imaging 51*, 42–50.

(12) La Bella, R., Garcia-Garayoa, E., Bahler, M., Blauenstein, P., Schibli, R., Conrath, P., Tourwe, D., and Schubiger, P. A. (2002) A ^{99m}Tc(I)-postlabeled high affinity bombesin analogue as a potential tumor imaging agent. *Bioconjugate Chem. 13*, 599–604.

(13) Smith, C. J., Gali, H., Sieckman, G. L., Higginbotham, C., Volkert, W. A., and Hoffman, T. J. (2003) Radiochemical investigations of ^{99m}Tc-N_3S-X-BBN[7−14]NH_2: An *in vitro/in vivo* structure-sctivity relationship study where X=0-, 3-, 5-, 8-, and 11-carbon tethering moieties. *Bioconjugate Chem. 14*, 93–102.

(14) Smith, C. J., Sieckman, G. L., Owen, N. K., Hayes, D. H., Mazuru, D. G., Kanna, R., Volkert, W. A., and Hoffman, T. J. (2003) Radiochemical investigations of gastrin-releasing peptide receptor specific [^{99m}Tc(X)(CO_3)-Dpr-Ser-Ser-Ser-Gln-Trp-Ala-Val-Gly-His-Leu-Met-(NH_2)] in PC-3, tumor-bearing, rodent models: syntheses, radiolabeling and *in vitro/vivo* studies where Dpr=2,3-diaminopropionic acid and X=H_2O or $P(CH_2OH)_3$. *Cancer Res. 63*, 4082–4088.

(15) Veerendra, B., Sieckman, G. L., Hoffman, T. J., Rold, T., Retzloff, L., and Smith, C. J. (2006) Synthesis, radiolabeling and in vitro GRP receptor targeting studies of ^{99m}Tc-Triaza-X-BBN[7−14]NH_2 (X=serylserylserine, glycylglycylglycine, glycylserylglycine, or beta alanine). *Synth. React. Inorg., Met.-Org., Nano-Met. Chem. 36*, 481–491.

(16) Alves, S., Paulo, A., Correia, J. D., Santos, I., Gano, L., Veerendra, B. C. J., Sieckman, G. L., Hoffman, T. J., Rold, T. L., Figueroa, S. D., Retzloff, L., McGrate, J., Prasanphanich, A., and Smith, C. J. (2006) Pyrazolyl conjugates of bombesin: a new tridentate ligand framework for the stabilization of fac-$[M(CO)_3]$+ moiety. *Nucl. Med. Biol. 33*, 625–634.

(17) Kunstler, J. U., Veerendra, B., Figueroa, S. D., Sieckman, G. L., Rold, T. L., Hoffman, T. J., Smith, L. C. J., and Pietzsch, H. J. (2007) Organometalic ^{99m}Tc(III) '4 + 1' bombesin(7−14) conjugates: synthesis, radiolabeling, and in vitro/in vivo studies. *Bioconjugate Chem. 18*, 1651–1661.

(18) Parry, J. J., Andrews, R., and Rogers, B. E. (2006) Micropet imaging of breast cancer using radiolabeled bombesin analogs targeting the gastrin-releasing peptide receptor. *Breast Cancer Res. Treat. 101*, 175–184.

(19) Parry, J. J., Kelly, T. S., Andrews, R., and Rogers, B. E. (2007) In vitro and in vivo evaluation of ^{64}Cu-labeled DOTA-linker-bombesin(7−14) analogues containing different amino acid linker moieties. *Bioconjugate Chem. 18*, 1110–1117.

(20) Rogers, B. E., Manna, D. D., and Savafy, A. (2004) In vitro and in vivo evaluation of a ^{64}Cu-labeled polyethylene glycol-bombesin conjugate. *Cancer Biother. Radiopharm. 19*, 25–34.

(21) Prasanphanich, A. F., Nanda, P. K., Rold, T. L., Ma, L., Lewis, M. R., Garrison, J. C., Hoffman, T. J., Sieckman, G. L., Figueroa, S. D., and Smith, C. J. (2007) [^{64}Cu-Nota-8-Aoc-BBN(7−14)NH_2] targeting vector for positron-emission tomography imaging of gastrin-releasing peptide receptor-expressing tissues. *Proc. Natl. Acad. Sci. U.S.A. 104*, 12462–12467.

(22) Schuhmacher, J., Zhang, H., Doll, J., Maecke, H. R., Matys, R., Hauser, H., Henze, M., Haberkorn, U., and Eisenhut, M. (2005) GRP receptor-targeted PET of a rat pancreas carcinoma xenograft in nude mice with a ^{68}Ga-labeled bombesin (6−14) analog. *J. Nucl. Med. 46*, 691–699.

(23) Zhang, X., Cai, W., Cao, F., Schreibmann, E., Wu, Y., Wu, J. C., Xing, L., and Chen, X. (2006) ^{18}F-Labeled bombesin analogs for targeting GRP receptor-expressing prostate cancer. *J. Nucl. Med. 47*, 492–501.

(24) Hoffman, T. J., Gali, H., Smith, C. J., Sieckman, G. L., Hayes, D. L., Owen, N. K., and Volkert, W. A. (2003) Novel series of ^{111}In-labeled

bombesin analogs as potential radiopharmaceuticals for specific targeting of gastrin-releasing peptide receptors expressed on human prostate cancer cells. *J. Nucl. Med. 44*, 823–831.

(25) Garrison, J. C., Rold, T. L., Sieckman, G. L., Naz, F., Sublett, S. V., Figueroa, S. D., Volkert, W. A., and Hoffman, T. J. (2008) Evaluation of the pharmacokinetic effects of various linking group using the ^{111}In-DOTA-X-BBN(7−14)NH_2 structural paradigm in a prostate cancer model. *Bioconjugate Chem. 19*, 1803–1812.

(26) Hu, F., Gutler, G. S., Hoffman, T. J., Sieckman, G. L., Volkert, W. A., and Jurisson, S. S. (2002) Pm-149 DOTA bombesin analogs for potential radiotherapy *In vivo* comparison with Sm-153 and Lu-177 labeled DO_3A-amide-β-Ala-BBN(7−14)NH_2. *Nucl. Med. Biol. 29*, 423–430.

(27) Zhang, H., Chen, J., Waldherr, C., Hinni, K., Waser, B., Reubi, J. C., and Maecke, H. R. (2004) Synthesis and evaluation of bombesin derivatives on the basis of pan-bombesin peptides labeled with indium-111, lutecium-177, and yttrium-90 for targeting bombesin receptor-expressing tumors. *Cancer Res. 64*, 6707–6715.

(28) Antunes, P., Ginj, M., Walter, M. A., Chen, J., Reubi, J. C., and Maecke, H. R. (2007) Influence of different spacers on the biological profile of a DOTA-somatostatin analogue. *Bioconjugate Chem. 18*, 84–92.

(29) Zhang, H., Schuhmacher, J., Waser, B., Wild, D., Eisenhut, M., Reubi, J. C., and Maecke, H. R. (2007) DOTA-PESIN, a DOTA-conjugated bombesin derivative designed for the imaging and targeted radionuclide treatment of bombesin receptor-positive tumors. *Eur. J. Nucl. Med. Mol. Imaging 34*, 1198–1208.

(30) Smith, C. J., Sieckman, G. L., Owen, N. K., Hayes, D. L., Mazuru, D. G., Volkert, W. A., and Hoffman, T. J. (2003) Radiochemical investigations of [^{188}Re(H_2O)$(CO)_3$-diamino propionic acid-SSS-bombesin(7−14)NH_2]: syntheses, radiolabeling and *in vitro*/*in vivo* GRP receptor targeting studies. *Anticancer Res. 23*, 63–70.

(31) Wong, E., Fauconnier, T., Bennett, S., Valliant, J., Nguyen, T., Lau, F., Lu, L. F. L., Pollak, A., Bell, R. A., and Thornback, J. R. (1997) Rhenium (V) and technetium (V) oxo complexes of an N_2NS peptidic chelator: evidence of interconversion between the syn and anti conformations. *Inorg. Chem. 36*, 5799–5808.

(32) Van de Wiele, C., Dumont, F., Vanden Broecke, R., Oosterlinck, W., Cocquyt, V., Serreyn, R., Peers, S., Thornback, J., Slegers, G., and Dierckx, R. A. (2000) Technetium-99m RP-527, a GRP analogue for visualization of GRP receptor-expressing malignancies: a feasibility study. *Eur. J. Nucl. Med. 27*, 1694–1699.

(33) Blok, D., Feitsma, H. I. J., Kooy, Y. M. C., Welling, M. M., Ossendorp, F., Vermeij, P., and Drijfhout, J. W. (2004) New chelation strategy allows for quick and clean ^{99m}Tc-labeling of synthetic peptides. *Nucl. Med. Biol. 31*, 815–820.

(34) Gourni, E., Paravatou, M., Bouziotis, P., Zikos, C., Fani, M., Xanthopoulos, S., Archimandritis, S. C., Livaniou, E., and Varvarigou, A. D. (2006) Evaluation of a series of new ^{99m}Tc-labeled bombesin-like peptides for early cancer detection. *Anticancer Res. 26*, 435–438.

(35) Gourni, E., Bouziotis, P., Zikos, C., Loudos, G., Xanthopoulos, S., Fani, M., Archimandritis, S. C., and Varvarigou, A. D. (2006) Comparative *in vivo* evaluation of two novel ^{99m}Tc-labeled bombesin derivatives. *Nucl. Instrum. Methods Phys. Res., Sect. A 569*, 518–521.

(36) Sarin, V. K., Kent, S. B. H., Tam, J. P., and Merrifield, R. B. (1981) Quantitative monitoring of solid phase peptide synthesis by the ninhydrin reaction. *Anal. Biochem. 117*, 147–157.

(37) Noll, B., Kniess, T., Friebe, M., Spies, H., and Johannsen, B. (1996) Rhenium $^{(V)}$ gluconate, a suitable precursor for the preparation of Rhenium$^{(V)}$ complexes. *Isot. Environ. Health Stud. 32*, 21–29.

(38) Varvarigou, A. D., Scopinaro, F., Leondiadis, L., Corleto, V., Schillaci, O., De Vincentis, G., Sourlingas, T. G., Sekeri-Pataryias, K. E., Enangelatos, G. P., Leonti, A., Xanthopoulos, S., Delle Fave, G., and Archimandritis, S. C. (2002) Synthesis, chemical, radiochemical and radiobiological evaluation of a new ^{99m}Tc-labeled bombesin-like peptide. *Cancer Biother. Radiopharm. 17*, 317–326.

(39) Nock, B., Nikolopoulou, A., Chiotellis, E., Loudos, G., Maintas, D., Reubi, J. C., and Maina, T. (2003) [^{99m}]Tc Demobesin 1, a novel potent bombesin analogue for GRP receptor-targeted tumor imaging. *Eur. J. Nucl. Med. 30*, 247–258.

(40) Alves, S., Paulo, A., Correia, J. D., Gano, L., Smith, C. J., Hoffman, T. J., and Santos, I. (2005) Pyrazolyl derivatives as bifunctional chelators for labeling tumor-seeking peptides with fac-[M(CO)3]+ Moiety (M=^{99m}Tc, Re): Synthesis, characterization, and biological behavior. *Bioconjugate Chem. 16*, 438–449.

(41) Okarvi, S. M. (2004) Peptide-based radiopharmaceuticals: future tools for diagnostic imaging of cancers and other diseases. *Med. Res. Rev. 24*, 357–397.

(42) Maecke, H. R. (2007) Radiolabeled peptides in Nuclear Oncology: Influence of Peptide Structure and Labeling Strategy on Pharmacology. *Molecular Imaging. Volume 49: An Essential Tool in Preclinical Research, Diagnostic Imaging and Therapy* (Bogdanor, A. A., Jr., Licha, K., Eds.) pp. 43−72, Chapter 10, Springer, Berlin, Germany.

(43) Prasanphanich, A. F., Lane, S. R., Figueroa, S. D., Ma, L., Rold, T. L., Sieckman, G. L., Hoffman, T. J., McCrate, J. M., and Smith, C. J. (2007) The effects of linking substituents on the *in vivo* behavior of site-directed, peptide-based, diagnostic radiopharmaceuticals. *In Vivo 21*, 1–16.

(44) Karra, S. R., Schibli, R., Gali, H., Katti, K. V., Hoffman, T. J., Higginbotham, C., Sieckman, G. L., and Volkert, W. A. (1999) ^{99m}Tc-Labeling and *in vivo* studies of a bombesin analogue with a novel water-soluble dithiaphosphine-based bifunctional chelating agent. *Bioconjugate Chem. 10*, 254–260.

(45) Dechristoforo, C., and Mather, S. J. (2002) The influence of chelator on the pharmacokinetics of ^{99m}Tc-labeled peptides. *Q. J. Nucl. Med. 46*, 195–205.

(46) Faintuch, B. L., Teodoro, R., Duatti, A., Muramoto, E., Faintuch, S., and Smith, C. J. (2008) Radiolabeled bombesin analogs for prostate cancer diagnosis: preclinical studies. *Nucl. Med. Biol. 35*, 401–411.

(47) Hohne, A., Mu, L., Honer, M., Schubiger, P. A., Ametamey, S. M., Graham, K., Stellfeld, T., Borkowski, S., Berndorff, D., Klar, U., Voigtmann, U., Cyr, J. E., Friebe, M., Dinkelborg, L., and Srinivasan, A. (2008) Synthesis, ^{18}F-labeling, and in vitro and in vivo studies of bombesin peptides modified with silicon-based building blocks. *Bioconjugate Chem. 19*, 1871–1879.

(48) Schweinsberg, C., Maes, V., Brans, L., Blauenstein, P., Tourwe, D. A., Schubiger, P. A., Schibli, R., and Garcia-Garayoa, E. (2008) Novel glycated [^{99m}Tc$(CO)_3$]-labeled bombesin analogues for improved targeting of Gastrin-releasing peptide receptor positive tumors. *Bioconjugate Chem. 19*, 2432–2439.

(49) Abd-Elgaliel, W. R., Gallazzi, F., Garrison, J. C., Rold, T. L., Sieckman, G. L., Figueroa, S. D., Hoffman, T. J., and Lever, S. Z. (2008) Design, synthesis and biological evaluation of an antagonist-bombesin analogue as targeting vector. *Bioconjugate Chem. 19*, 2040–2048.

(50) Cescato, R., Maina, T., Nock, B., Nikolopoulou, A., Charalambidis, D., Piccand, V., and Reubi, J. C. (2008) Bombesin receptor antagonists may be preferable to agonists for tumor imaging. *J. Nucl. Med. 49*, 318–326.

(51) Lambert, B., Cybulla, M., Weiner, S. M., Van De Wiele, C., Ham, H., Dierckx, R. A., and Otte, A. (2004) Renal toxicity after radionuclide therapy. *Radiat. Res. 161*, 607–611.

(52) Behe, M., Kluge, G., Becker, W., Gotthardt, M., and Behr, T. M. (2005) Use of polyglutamic acids to reduce uptake of radiometal-labeled minigastrin in the kidneys. *J. Nucl. Med. 46*, 1012–1015.

(53) Garcia-Garayoa, E., Schweinsberg, C., Maes, V., Brans, L., Blauenstein, P., Tourwe, D. A., Schibli, R., and Schubiger, P. A. (2008) Influence of molecular charge on the biodistribution of bombesin analogues labeled with the [^{99m}Tc$(CO)_3$]-core. *Bioconjugate Chem. 19*, 2409–2416.

(54) Akizawa, H., Uehara, T., and Arano, Y. (2008) Renal uptake and metabolism of radiopharmaceuticals derived from peptides and proteins. *Adv. Drug Delivery Rev. 60*, 1319–1328.

(55) Akizawa, H., Arano, Y., Mifune, M., Iwado, A., Saito, Y., Mukai, T., Uehara, T., Ono, M., Fujioka, Y., Ogawa, K., Kiso, Y., and Saji, H. (2001) Effect of molecular charges on renal uptake and metabolism of ^{111}In-DTPA-conjugated peptides. *Nucl. Med. Biol. 28*, 761–768.

(56) Chapman, A. P. (2002) PEGylated antibodies and antibody fragments for improved therapy: a review. *Adv. Drug Delivery Rev. 54*, 531–545.

BC800475K